
Debona: Decoupled Boundary Network Analysis for Tighter Bounds and Faster Adversarial Robustness Proofs

Christopher Brix

Software Modeling and Verification Group
RWTH Aachen University
Aachen, D-52074
christopher.brix@rwth-aachen.de

Thomas Noll

Software Modeling and Verification Group
RWTH Aachen University
Aachen, D-52074
noll@cs.rwth-aachen.de

Abstract

Neural networks are commonly used in safety-critical real-world applications. Unfortunately, the predicted output is often highly sensitive to small, and possibly imperceptible, changes to the input data. Proving that either no such adversarial examples exist, or providing a concrete instance, is therefore crucial to ensure safe applications. As enumerating and testing all potential adversarial examples is computationally infeasible, verification techniques have been developed to provide mathematically sound proofs of their absence using overestimations of the network activations. We propose an improved technique for computing tight upper and lower bounds of these node values, based on increased flexibility gained by computing both bounds independently of each other. Furthermore, we gain an additional improvement by re-implementing part of the original state-of-the-art software “Neurify”, leading to a faster analysis. Combined, these adaptations reduce the necessary runtime by up to 78%, and allow a successful search for networks and inputs that were previously too complex. Finally, we provide proofs for tight upper and lower bounds on max-pooling layers in convolutional networks. To ensure widespread usability, we open source our implementation “Debona”, featuring both the implementation specific enhancements as well as the refined boundary computation for faster and more exact results.

1 Introduction

Major advances in both the theory and implementation of neural networks have enabled their employment in many application domains including safety-critical ones, such as autonomous driving [Bojarski et al., 2016], healthcare [Esteva et al., 2019], or military [Wu et al., 2015]. However, experience shows that neural networks often lack *robustness* properties, meaning that small, or even imperceptible, perturbations of a correctly classified input can make it misclassified [Szegedy et al., 2013]. Such *adversarial examples* have raised serious concerns as classification failures can entail severe consequences especially in safety-critical applications.

To overcome this problem, two approaches can be taken that complement each other. The first one is to guide the training process of neural networks so as to improve their robustness. This can be accomplished, e.g., by incorporating relaxation methods [Dvijotham et al., 2018a, Wong et al., 2018]. The second approach is to verify the safety of the trained network by providing evidence for the absence of adversarial examples. For this purpose, heuristic search techniques have been developed that are based on gradient descent [Carlini and Wagner, 2017, Szegedy et al., 2013], evolutionary algorithms [Nguyen et al., 2015], or saliency maps [Papernot et al., 2016]. However, such methods usually do not provide reliable correctness assertions as they can only show the presence of adversarial examples but never their absence.

For safety-critical applications, however, it is required that robustness properties of neural networks are rigorously established. Therefore, techniques based on formal verification have been developed to prove the absence of adversarial examples within a certain distance of a given input. Ideally, an automated algorithm should either guarantee that this property is satisfied by the network or find concrete counterexamples demonstrating its violation. The effectiveness and efficiency of such automated approaches crucially depends on how precisely they can estimate the decision boundary of the network. This is known to be a hard problem for networks with piecewise linear activation functions, such as ReLUs [Montufar et al., 2014]. While the activation function of each node can be decomposed into its linear segments, the number of their possible combinations increases exponentially with the number of nodes. Therefore, performing the analysis by exhaustively enumerating these combinations is intractable.

The key idea to combat this state-space explosion problem is to apply *over-approximation* by means of symbolic techniques. Symbolic representations allow to keep track of dependencies across network layers when the actual dependencies become too complex to be represented explicitly. One of the most promising approaches of this kind is introduced in [Wang et al., 2018a] and implemented in the Neurify tool¹, combining symbolic interval analysis, linear relaxation, and constraint refinement to iteratively minimize the errors introduced during the relaxation process. As we will see later, however, this approach makes the assumption that the interval bounds established by symbolic relaxation differ by a constant amount. In many cases, this entails inaccuracies that could be avoided by obtaining tighter bounds through an independent and, thus, more flexible handling of these bounds.

The contribution of the present paper is to introduce such an enhancement. Its key idea is to exploit the fact that when using ReLU activation functions, the value of a node is at least zero. This can help to improve lower bounds with an otherwise weak estimate, and subsequently also allows to tighten upper bounds. Furthermore, we re-implemented part of Neurify, leading to a faster analysis. By exploiting both the implementation-specific improvements and the computation of tighter bounds, our software “Debona” reduces the runtime of analyses by up to 78%, and increases the rate of successful analyses significantly. Finally, we provide proofs for tight upper and lower bounds on max-pooling layers in convolutional networks. We open source Debona, to make it publicly available.²

The remainder of this paper is structured as follows. After giving a brief overview of related work and of preliminaries in Sections 2 and 3, we detail the analysis techniques implemented by Neurify and our own improvements in Sections 4 and 5, respectively. The setup for assessing the latter and the outcomes of the evaluation are described in Section 6, followed by a short conclusion in Section 7.

2 Related work

In this section, we focus on symbolic techniques for formal safety analyses of given neural networks, ignoring approaches such as heuristic search algorithms or robustness-oriented training. Verification methods include constraint solving based on Satisfiability Modulo Theories (SMT) reasoning [Dvijotham et al., 2018b, Ehlers, 2017, Katz et al., 2017, Lomuscio and Maganti, 2017, Narodytska et al., 2018, Pulina and Tacchella, 2010, Wong and Kolter, 2018] or Mixed Integer Linear Programming (MILP) solvers [Dutta et al., 2018, Fischetti and Jo, 2017, Tjeng et al., 2019], layer-by-layer exhaustive search [Huang et al., 2017, Weng et al., 2018], and global optimization [Ruan et al., 2018]. Unfortunately, the efficiency of these techniques is usually impaired by the high degree of nonlinearity of the resulting formulae.

To overcome this problem, several linear or convex relaxation methods have been developed to strictly approximate the decision boundary of a network, notably those based on abstract interpretation [Li et al., 2019, Gehr et al., 2018, Singh et al., 2018, 2019]. While they tend to scale better than solver-based approaches, this often comes at the price of reduced precision, entailing high false positive rates and problems with identifying real counterexamples that substantiate violations of safety properties.

Our approach directly builds on the work described in [Wang et al., 2018a], which proposes a combined approach that essentially employs symbolic relaxation techniques to identify crucial nodes and that iteratively refines output approximations over these nodes with the help of a linear solver.

¹<https://github.com/tcwangshiqi-columbia/Neurify>

²<https://github.com/ChristopherBrix/Debona>

3 Notation

For a given neural network, let the size of the input layer be denoted by s_0 , followed by n subsequent fully connected feed-forward layers of size s_1, \dots, s_n . The node values $\hat{x}_1^{(0)}, \dots, \hat{x}_{s_0}^{(0)}$ of the input nodes represent the network input. Node inputs in subsequent layers are computed as the weighted sum $x_i^{(l)} = \sum_{j=1}^{s_{l-1}} w_{i,j} \cdot \hat{x}_j^{(l-1)}$. For all intermediate layers, the node output $\hat{x}_i^{(l)}$ is computed by applying a non-linear activation function g : $\hat{x}_i^{(l)} = g(x_i^{(l)})$. Even though different activation functions exist, this work assumes only ReLU operations are used, i.e., $\hat{x}_i^{(l)} = \max\{0, x_i^{(l)}\}$, as they are easy to compute, piecewise-linear, and commonly used. The propagation is stopped once the network output $x_i^{(n)}$ is computed. For notational simplicity, $x_i^{(l)}$ and $\hat{x}_i^{(l)}$ are referred to as x and \hat{x} whenever the specific i and l are not important.

Eq^* is the higher order function returning the non-linear formula for a given node x . Each node can be approximated by linear upper and lower bounds. These will be referred to as $Eq_{up}(x)$ and $Eq_{low}(x)$, respectively. Determining the bounds as a function, as opposed to a simple interval, reduces the overestimation error (see Section 4). For the range of valid inputs, specified by the concrete example and its maximal perturbation, both bounds have minimal and maximal values $\overline{Eq_{low}(x)}, \underline{Eq_{up}(x)}$ and $\overline{Eq_{low}(x)}, \underline{Eq_{up}(x)}$, respectively. Wherever a distinction of upper and lower bound is not necessary for the given argument, as it holds for both instances, they are referred to as $Eq(x)$. All listed equations can be determined for \hat{x} as well.

4 Neurify

For input nodes, upper and lower bounds are determined as a direct result of the given input and the defined L_∞ value for possible manipulations. Other commonly used bounds like L_1 and L_2 [Goodfellow et al., 2015] are supported as well, but not discussed in this paper. Based on the input bounds, Neurify [Wang et al., 2018a] uses *symbolic propagation* to determine the bounds for each following node. As opposed to naive interval propagation, symbolic propagation allows to detect common factors of equations, and therefore to tighten the computed bounds:

$$a \in [0, 1] \Rightarrow a - 0.5a \stackrel{\text{interval}}{\in} [0, 1] - 0.5 \cdot [0, 1] = [0, 1] - [0, 0.5] = [-0.5, 1] \quad (1)$$

$$a \in [0, 1] \Rightarrow a - 0.5a \stackrel{\text{symbolic}}{=} 0.5a \in [0, 0.5] \quad (2)$$

Due to the ReLU operations used as the non-linear activation function, the computed symbolic bounds may have to be relaxed to correctly bound the output of each node. Wang et al. [2018a] identify three regions the node's bound $Eq(x)$ may fall into:

1. $0 \leq \underline{Eq(x)} \leq \overline{Eq(x)}$: If the lowest value taken by the bound is already non-negative, the ReLU operation has no effect on it, and therefore $Eq(\hat{x}) = Eq(x)$.
2. $\underline{Eq(x)} \leq \overline{Eq(x)} \leq 0$: If the largest value the bound may take is non-positive, the ReLU operation guarantees that $Eq(\hat{x}) = 0$.
3. $\underline{Eq(x)} \leq 0 \leq \overline{Eq(x)}$: If the boundary indicates that the node may become both negative and positive, there is a non-linear dependence between the node's input and output. Thus, the output bounds need to be relaxed. Wang et al. [2018a] refer to these nodes as *overestimated*.

For overestimated nodes, they propose to use *symbolic linear relaxation* to find new bounds for the ReLU output that are valid, but still tight. They prove that the relaxations

$$Eq_{up}(\hat{x}) = Relax(\max\{0, Eq_{up}(x)\}) = \frac{\overline{Eq_{up}(x)}}{\overline{Eq_{up}(x)} - \underline{Eq_{up}(x)}} (Eq_{up}(x) - \underline{Eq_{up}(x)}) \quad (3)$$

$$Eq_{low}(\hat{x}) = Relax(\max\{0, Eq_{low}(x)\}) = \frac{\overline{Eq_{low}(x)}}{\overline{Eq_{low}(x)} - \underline{Eq_{low}(x)}} Eq_{low}(x) \quad (4)$$

minimize the maximal distance between $\max\{0, Eq(x)\}$ and $Eq(\hat{x})$. This relaxation is visualized in Figures 1 and 2. However, as shown in Section 5.1, it is not optimal for approximating $Eq^*(\hat{x})$.

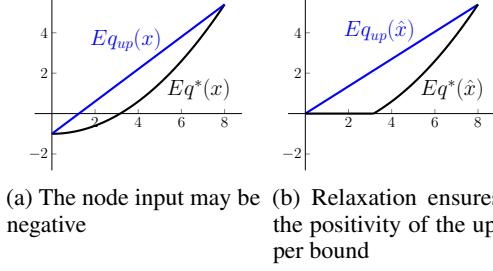


Figure 1: Relaxation of the upper bound is mandatory

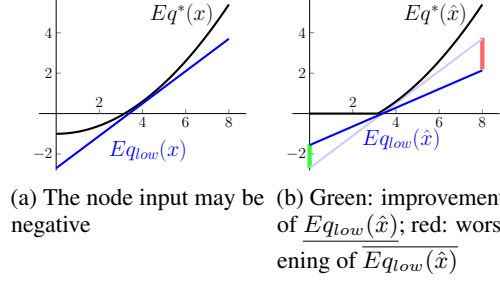


Figure 2: Relaxation of the lower bound is optional and a trade off

Neurify makes the additional assumption that both bounds are separated only by some scalar δ , i.e.:

$$Eq_{up}(x) = g(x) + \delta_{up}^x \quad (5)$$

$$Eq_{low}(x) = g(x) + \delta_{low}^x \quad (6)$$

As this implies that the upper and lower bounds cannot be adapted individually, Wang et al. [2018a] simplify Equations 3 and 4 by overestimating $Eq_{up}(x) \geq \overline{Eq_{low}(x)}$ and $\overline{Eq_{low}(x)} \leq \overline{Eq_{up}(x)}$. This ensures that both bounds are scaled by the same amount, yielding

$$Eq_{up}(\hat{x}) = g(\hat{x}) + \delta_{up}^{\hat{x}} = \frac{\overline{Eq_{up}(x)}}{\overline{Eq_{up}(x)} - \overline{Eq_{low}(x)}} (g(x) + \delta_{up}^x - \overline{Eq_{low}(x)}) \quad (7)$$

$$Eq_{low}(\hat{x}) = g(\hat{x}) + \delta_{low}^{\hat{x}} = \frac{\overline{Eq_{up}(x)}}{\overline{Eq_{up}(x)} - \overline{Eq_{low}(x)}} (g(x) + \delta_{low}^x) \quad (8)$$

However, it introduces an overestimation, implying that the resulting bounds are no longer maximally tight. As described in Section 5, it is theoretically possible to determine better estimations of $\overline{Eq_{up}(x)}$, and decoupling the bounds allows to improve the lower bound significantly.

At each node, the upper (lower) bound is determined as the weighted sum of the upper (lower) bound of all previous nodes with a positive weight plus the weighted sum of the lower (upper) bound of all previous nodes with a negative weight.

$$Eq_{up}(x_j^{(l+1)}) = \sum_{i \in [1, \dots, s_l], w_{j,i} > 0} w_{j,i} \cdot Eq_{up}(\hat{x}_i^{(l)}) + \sum_{i \in [1, \dots, s_l], w_{j,i} < 0} w_{j,i} \cdot Eq_{low}(\hat{x}_i^{(l)}) \quad (9)$$

However, a naive application of this approach leads to weakened bounds. For $l_i(x) \leq f_i(x) \leq u_i(x) \forall i \in [1, 3]$, $f_2(x) = -\frac{1}{2}f_1(x)$, and $f_3(x) = f_1(x) + f_2(x)$, the bounds of f_3 could be computed as

$$u_3(x) = u_1(x) + u_2(x) = u_1(x) - \frac{1}{2}l_1(x) \quad (10)$$

$$l_3(x) = l_1(x) + l_2(x) = l_1(x) - \frac{1}{2}u_1(x) \quad (11)$$

even though $f_3(x) = f_1(x) + f_2(x) = f_1(x) - \frac{1}{2}f_1(x) = \frac{1}{2}f_1(x)$ and therefore

$$u_3(x) = \frac{1}{2}u_1(x) \leq u_1(x) - \frac{1}{2}l_1(x) \quad (12)$$

$$l_3(x) = \frac{1}{2}l_1(x) \geq l_1(x) - \frac{1}{2}u_1(x) \quad (13)$$

Thus, it is important to track different paths that lead to the same node to first simplify the underlying equation as much as possible, before determining the new upper and lower bounds. Even though this is not described in [Wang et al., 2018a], it is implemented in Neurify.

After bounds for all nodes have been computed, Neurify uses an LP solver to find a potential adversarial example. If evaluating the concrete input invalidates it, Neurify splits an overestimated node and performs separate analyses for the assumption that it is either positive, or zero. Therefore, in both these sub-analyses, no overestimation of the given node is necessary, and the bounds are tightened. Wang et al. [2018a] split those nodes first that have the highest output gradient, an approach proposed by Wang et al. [2018b].

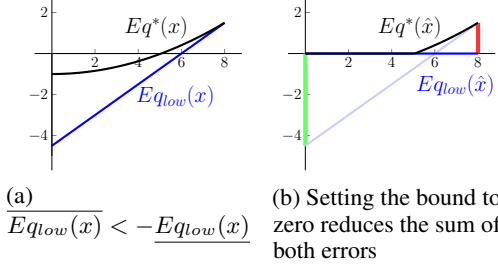


Figure 3: Zero bounding

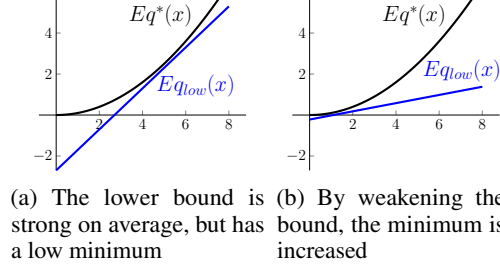


Figure 4: Maximizing the minimal lower bound

5 Improvements

The proposed improvements over Neurify are two-fold: First, we provide Debona 1.0 as a re-implementation of parts of Neurify that eliminates some bugs from the original version. We note that those bugs prevent Neurify from providing a mathematically sound proof for the (non-)existence of some adversarial examples. For the inputs analyzed in this work, Neurify wrongly returns “no adv. ex.” for two out of the 6,000 performed analyses, even though an adversarial example provably exists. Moreover, Debona 1.0 avoids some performance bottlenecks, leading to a significantly faster analysis. Notably, Debona makes full use of all available threads by performing a parallel search over possible splits, whereas Neurify may occasionally not use the full power of parallelization. Debona also aborts the LP solver after 30 seconds, to avoid long delays due to unfavorable network constraints. In those situations, the analysis proceeds with the next split. Those optimizations allow the successful analysis of inputs and networks that previously resulted in a timeout or abortion. The correctness of Debona has been verified by comparing the analysis results with the equivalent but slower Neurify version.

Further speedups are realized by determining tighter bounds on the network nodes. By reducing the overestimation, less splits have to be performed until an adversarial example can be found, or their absence can be proven. As weak bounds in early layers negatively influence the bounds of later layers, tight approximations are especially important for deep networks. The major improvement of Debona 1.1 over Neurify is the ability to reduce the approximation error by defining the upper and lower bounds independently of each other. As described in Section 4, Neurify computes one function $g(x)$ for each node x , and computes the upper and lower bounds as $g(x) + \delta_{up}^x$ and $g(x) + \delta_{low}^x$, respectively. This implies that the lower bound cannot be changed (other than by moving it up or down by a scalar δ) without influencing the upper bound as well. For decoupled bounds, we prove the existence of a tighter lower bound, resulting in overall tighter approximations.

In addition to the improvements gained by decoupling the upper and lower bounds, we propose an extension of the analysis that enables the efficient computation of tight bounds for max-pooling layers, under the requirement that each such layer is preceded by a ReLU operation.

5.1 Zero bounding

Wang et al. [2018a] prove that Equation 4 minimizes the maximal distance between $\max\{0, Eq_{low}(x)\}$ and $Eq_{low}(\hat{x})$. However, we argue that the lower bound $Eq_{low}(\hat{x})$ should be chosen such that

$$Eq_{low}(\hat{x}) = \arg \min_{Eq_{low}(\hat{x})} \{(\max\{0, Eq_{low}(x)\} - Eq_{low}(\hat{x})) + (\max\{0, Eq_{low}(x)\} - \overline{Eq_{low}(\hat{x})})\} \quad (14)$$

$$= \arg \min_{Eq_{low}(\hat{x})} \{0 - \overline{Eq_{low}(\hat{x})} + \overline{Eq_{low}(x)} - \overline{Eq_{low}(\hat{x})}\} \quad (15)$$

$$= \arg \min_{Eq_{low}(\hat{x})} \{-\overline{Eq_{low}(\hat{x})} - \overline{Eq_{low}(\hat{x})}\} \quad (16)$$

where the last transformation is valid as $\overline{Eq_{low}(x)}$ is constant with respect to $Eq_{low}(\hat{x})$. We highlight that this represents the sum of the maximum error on both the positive and the negative regime of the bound, whereas Wang et al. [2018a] minimize the maximum of both errors. By minimizing the sum, we allow the bound estimation to perform a trade off between optimizing both errors, reducing the overall overestimation.

Because the lower bound must be a linear equation, $Eq_{low}(\hat{x}) = m \cdot Eq_{low}(x) + n$. Therefore

$$\begin{aligned} Eq_{low}(\hat{x}) &= \arg \min_{m \cdot Eq_{low}(x) + n} \{ -m \cdot Eq_{low}(x) + n - \overline{m \cdot Eq_{low}(x) + n} \} \\ &= \arg \max_{m \cdot Eq_{low}(x) + n} \{ \overline{m \cdot Eq_{low}(x) + n} + m \cdot Eq_{low}(x) + n \} \end{aligned}$$

In the positive region of the bound, $Eq_{low}(\hat{x})$ must not provide stronger estimates than $Eq_{low}(x)$, i.e., $Eq_{low}(\hat{x})|_{Eq_{low}(x) \geq 0} \leq Eq_{low}(x)|_{Eq_{low}(x) \geq 0}$, and both $\underline{Eq_{low}(\hat{x})}$ and $\overline{Eq_{low}(\hat{x})}$ are to be maximized. Therefore, $n = 0$ and $0 \leq m \leq 1$. It follows

$$\begin{aligned} Eq_{low}(\hat{x}) &= \arg \max_{m \cdot Eq_{low}(x)} \{ \overline{m \cdot Eq_{low}(x)} + m \cdot Eq_{low}(x) \} \\ &= \arg \max_{m \cdot Eq_{low}(x)} \{ m \cdot (\underline{Eq_{low}(x)} + \overline{Eq_{low}(x)}) \} \\ &= \begin{cases} Eq_{low}(x), & \text{if } \underline{Eq_{low}(x)} + \overline{Eq_{low}(x)} \geq 0 \\ 0, & \text{otherwise} \end{cases} \end{aligned}$$

Thus, Debona keeps the lower bound unchanged unless $\underline{Eq_{low}(x)} + \overline{Eq_{low}(x)} < 0$, in which case it is replaced with a constant boundary of zero. We refer to this process as *zero bounding*. The tightened lower bound positively impacts both the positive and negative bounds of subsequent layers. A visualization of zero bounding is shown in Figure 3.

5.2 Over-approximation of upper bounds

As described in Section 4, the upper bound needs to be relaxed if it could be negative. To this end, $\underline{Eq_{up}(x)}$ and $\overline{Eq_{up}(x)}$ have to be computed. For $\underline{Eq_{up}(x)}$, $Eq_{low}(x)$ as used by Neurify is a valid over-approximation. However, many possible lower bounds $\underline{Eq_{low}(x)}$ exist, and the one chosen to determine $\underline{Eq_{up}(x)}$ may be different from bounds on x for other purposes. Specifically, it may be beneficial to trade a weaker overall bound for an increased minimum. A visualization of this trade off is shown in Figure 4. Empirically, however, we notice that the increased computational overhead does not justify the improved boundary accuracy, and therefore, Debona does not use this optimization technique.

5.3 Max-pooling

Convolutional networks commonly use max-pooling layers to reduce the layer size, which introduces additional non-linearity. For a max-pooling operation $\max\{x_j^{(l)}, \dots, x_{j+k}^{(l)}\}$ we propose the following upper and lower bounds:

$$\max\{Eq_{up}(x_j^{(l)}), \dots, Eq_{up}(x_{j+k}^{(l)})\} \quad (17)$$

$$= \max\left\{ \sum_{\substack{i \in [1, s_{l-1}], \\ w_{j,i} > 0}} w_{j,i} \cdot Eq_{up}(\hat{x}_i^{(l-1)}) + \sum_{\substack{i \in [1, s_{l-1}], \\ w_{j,i} < 0}} w_{j,i} \cdot \tilde{Eq}_{low}(\hat{x}_i^{(l-1)}), \dots, \right. \quad (18)$$

$$\left. \sum_{\substack{i \in [1, s_{l-1}], \\ w_{j+k,i} > 0}} w_{j+k,i} \cdot Eq_{up}(\hat{x}_i^{(l-1)}) + \sum_{\substack{i \in [1, s_{l-1}], \\ w_{j+k,i} < 0}} w_{j+k,i} \cdot \tilde{Eq}_{low}(\hat{x}_i^{(l-1)}) \right\} \\ \leq \max\left\{ \sum_{\substack{i \in [1, s_{l-1}], \\ w_{j,i} > 0}} w_{j,i} \cdot Eq_{up}(\hat{x}_i^{(l-1)}), \dots, \sum_{\substack{i \in [1, s_{l-1}], \\ w_{j+k,i} > 0}} w_{j+k,i} \cdot Eq_{up}(\hat{x}_i^{(l-1)}) \right\} \quad (19)$$

$$\leq \sum_{i \in [1, s_{l-1}]} \max\{w_{j+r,i} \mid r \in [0, k], w_{j+r,i} > 0\} \cdot Eq_{up}(\hat{x}_i^{(l-1)}) \quad (20)$$

$$= \sum_{i \in [1, s_{l-1}]} \max\{w_{j,i}, \dots, w_{j+k,i}, 0\} \cdot Eq_{up}(\hat{x}_i^{(l-1)}) \quad (21)$$

$$\min\{Eq_{low}(x_j^{(l)}), \dots, Eq_{low}(x_{j+k}^{(l)})\} \quad (22)$$

$$\stackrel{\text{analogous}}{\geq} \sum_{i \in [1, s_i]} \min\{w_{j,i}, \dots, w_{j+k,i}, 0\} \cdot Eq_{up}(\hat{x}_i^{(l-1)}) \quad (23)$$

where $\tilde{Eq}_{low}(\hat{x}_i^{(l-1)}) = \max\{0, Eq_{low}(\hat{x}_i^{(l-1)})\}$ is a valid tightened lower bound if layer $l - 1$ uses ReLUs as the activation function. We propose to implement and evaluate those bounds in future work.

5.4 Performance analysis

As described in Section 4, it is important to accumulate the effect of each predecessor node over all possible network paths, to avoid weakening the upper and lower bounds. We note that Neurify is able to do this as part of the forward propagation of bounds, yielding an analysis in $\mathcal{O}(n \cdot \max_{i \in [0, n]} s_i)$ steps. Due to the decoupled bounds, and therefore complicated equation storage, Debona cannot efficiently do so. Thus, possible paths through the network need to be traced back from the current node to the input layer, increasing the cost of analysis to $\mathcal{O}(n^2 \cdot \max_{i \in [0, n]} s_i)$. However, as shown in Section 6, the actual overall runtime is still improved.

6 Experimental evaluation

We perform a series of experiments to show both the implementation specific improvements of Debona 1.0 over Neurify and the additional improvements gained through the decoupling of upper and lower bounds as described in Section 5 and implemented in Debona 1.1.

For all three software implementations, we evaluate images on six different networks: ff2x24, ff2x50, ff2x512, ff3x24, ff3x50, and ff5x24 are feed-forward networks with the specified number and sizes of hidden layers (i.e., a network structure of e.g. $784 \times 24 \times 24 \times 10$ for ff2x24). Networks ff2x24, ff2x50 and ff2x512 are the same as those used in [Wang et al., 2018a]. Networks ff3x24, ff3x50 and ff5x24 are trained on the MNIST corpus [LeCun et al., 2010] for six epochs, using Adam [Kingma and Ba, 2015] with a learning rate of 0.001. We note that we do not strive for strong network performance, nor do we train the networks to make them more robust against adversarial attacks, as the aim of this work is solely to demonstrate the effectiveness of the analyses.

All analyses are run on a machine with eight cores and 16 GB RAM. If the analysis has not terminated after one hour (i.e., no adversarial example has been found, but the network has also not been proven to be robust), it is aborted. For each experiment, we test for adversarial examples against 1,000 test images from the MNIST dataset for a maximal input perturbation of $L_\infty = 10$ and report the average wall-clock time spent on a single image, as well as the number of splits performed. Both values are averaged over the common subset of the 1,000 test images that could be successfully analyzed by Neurify, Debona 1.0 and Debona 1.1. Images that lead to a timeout or error for one of these implementations were excluded from the average, as the timeout of one hour was arbitrarily chosen, and including them would distort the average. A complete list of all detailed results is given in the appendix. All experiments are performed using double precision floating point operations. We note that the results for Neurify are not completely consistent across repeated executions, as bugs in the implementation may cause race-conditions. The reported values are selected from a random run, so the average results are representative.

The results in Table 1 show significant gains both by the implementation specific improvements in Debona 1.0, and the additionally tightened bounds in Debona 1.1. Across all networks, the average runtime decreases by 16–51% when switching to Debona 1.0, demonstrating the importance of highly efficient code. Even though our optimizations enable maximal parallelism and reduce other bottlenecks, we propose to further optimize the implementation for additional gains. By open sourcing Debona, we hope to stimulate such development.

Debona 1.1 provides an additional 22–72% reduction in runtime. This improvement is solely based on our proposed technique, zero bounding, enabled by the decoupling of the computation of the upper and lower bounds. With a combined decrease in runtime of 62–78%, Debona 1.1 allows to test for adversarial examples up to four times as fast as the previous state-of-the-art software Neurify. Furthermore, it enables the analysis of networks and inputs that were previously too complex. While the decrease in unsuccessful analyses from Neurify to Debona 1.0 is based both on our removal

Table 1: Performance of analyses

Network	Software	Time [s]	Sub-analyses	Analysis result		
				adv.	non-adv.	undetermined
ff2x24	Neurify	4.7	141	770	222	8
	Debona 1.0	2.3 (−51%)	126 (−11%)	773	227	0 (−100%)
	Debona 1.1	1.8 (−62%)	98 (−30%)	773	227	0 (−100%)
ff2x50	Neurify	85.1	2,677	663	213	126
	Debona 1.0	51.8 (−39%)	2,786 (+4%)	671	238	91 (−28%)
	Debona 1.1	21.5 (−75%)	1,207 (−55%)	673	254	73 (−42%)
ff2x512	Neurify	4.1	65	252	11	737
	Debona 1.0	3.1 (−24%)	66 (+2%)	253	16	731 (−1%)
	Debona 1.1	0.9 (−78%)	3 (−95%)	224	57	719 (−2%)
ff3x24	Neurify	17.7	454	603	371	26
	Debona 1.0	8.8 (−50%)	398 (−12%)	608	391	1 (−96%)
	Debona 1.1	6.8 (−62%)	302 (−33%)	608	391	1 (−96%)
ff3x50	Neurify	133.7	3,681	561	215	224
	Debona 1.0	91.9 (−31%)	3,574 (−3%)	561	255	184 (−18%)
	Debona 1.1	29.1 (−78%)	1,229 (−67%)	558	289	153 (−32%)
ff5x24	Neurify	91.9	2,434	677	244	79
	Debona 1.0	77.6 (−16%)	1,981 (−19%)	689	262	49 (−38%)
	Debona 1.1	33.7 (−63%)	1,160 (−52%)	693	272	35 (−65%)

of bugs that cause the analysis to fail or miss critical regions of the search space, and the general speedup, Debona 1.1 provides tighter upper and lower estimations for each node, thus significantly reducing the complexity of the search. An overview of the bound tightness is given in the appendix.

We highlight that Debona 1.1 performs better for the detection of proofs for the non-existence of adversarial examples than for finding specific non-safe instances. For networks ff2x512 and ff3x50, the number of found adversarial examples decreases, while the number of provenly safe inputs significantly increases. This indicates that while the tightened bounds reduce the search space sufficiently to prove that many networks are robust to adversarial attacks, for some inputs adversarial examples exist but are hidden in a large search space. As the improved boundaries influence the search pattern, previously reachable instances may be moved back too far, causing a timeout. We propose to further investigate this effect, to find search patterns that are robust to changes in the network boundaries and to speed up the detection of adversarial examples.

7 Conclusion

In conclusion, we have shown that by decoupling the computation of the upper and lower bound, significant improvements to the network boundary estimation can be realized. We have proven that zero bounding allows for overall tighter approximations of the lower bound by jointly optimizing its error in both the negative and positive regime. In our open source implementation, we gain a speedup of up to 78% by applying this technique in combination with implementation-specific modifications, compared with the state-of-the-art software Neurify. Furthermore, we provide the formula for tight upper and lower bounds on max-pooling layers, proposing their implementation and evaluation as future work.

Broader impact

By providing mathematically sound proofs for the non-existence of adversarial examples, Debona may help to justify the application of neural networks in safety-critical applications. While increased trust and control is generally desirable, it is important to note that Debona only disproves the existence of adversarial examples for a given input, not for any possible input, and that the network prediction should still be handled with care. Given full access to a network and its weights, Debona may also be used by attackers to actively search for adversarial examples and maliciously fool a network.

References

- Mariusz Bojarski, Davide Del Testa, Daniel Dworakowski, Bernhard Firner, Beat Flepp, Praseem Goyal, Lawrence D. Jackel, Mathew Monfort, Urs Muller, Jiakai Zhang, Xin Zhang, Jake Zhao, and Karol Zieba. End to end learning for self-driving cars. *CoRR*, abs/1604.07316, 2016. URL <http://arxiv.org/abs/1604.07316>.
- Andre Esteva, Alexandre Robicquet, Bharath Ramsundar, Volodymyr Kuleshov, Mark DePristo, Katherine Chou, Claire Cui, Greg Corrado, Sebastian Thrun, and Jeff Dean. A guide to deep learning in healthcare. *Nature medicine*, 25(1):24–29, 2019. doi: 10.1038/s41591-018-0316-z.
- H. Wu, H. Zhang, J. Zhang, and F. Xu. Typical target detection in satellite images based on convolutional neural networks. In *2015 IEEE International Conference on Systems, Man, and Cybernetics*, pages 2956–2961. IEEE, 2015. doi: 10.1109/SMC.2015.514.
- Christian Szegedy, Wojciech Zaremba, Ilya Sutskever, Joan Bruna, Dumitru Erhan, Ian Goodfellow, and Rob Fergus. Intriguing properties of neural networks. *CoRR*, abs/1312.6199v4, 2013. URL <http://arxiv.org/abs/1312.6199v4>.
- Krishnamurthy Dvijotham, Sven Gowal, Robert Stanforth, Relja Arandjelovic, Brendan O’Donoghue, Jonathan Uesato, and Pushmeet Kohli. Training verified learners with learned verifiers. *CoRR*, abs/1805.10265, 2018a. URL <http://arxiv.org/abs/1805.10265>.
- Eric Wong, Frank Schmidt, Jan Hendrik Metzen, and J. Zico Kolter. Scaling provable adversarial defenses. In *Advances in Neural Information Processing Systems 31*, pages 8400–8409. Curran Associates, Inc., 2018. URL <http://papers.nips.cc/paper/8060-scaling-provable-adversarial-defenses.pdf>.
- Nicholas Carlini and David Wagner. Towards evaluating the robustness of neural networks. In *2017 IEEE Symposium on Security and Privacy (SP)*, pages 39–57. IEEE, 2017. doi: 10.1109/SP.2017.49.
- Anh Nguyen, Jason Yosinski, and Jeff Clune. Deep neural networks are easily fooled: High confidence predictions for unrecognizable images. In *2015 IEEE Conference on Computer Vision and Pattern Recognition (CVPR)*, pages 427–436. IEEE, 2015. doi: 10.1109/CVPR.2015.7298640.
- Nicolas Papernot, Patrick McDaniel, Somesh Jha, Matt Fredrikson, Z. Berkay Celik, and Ananthram Swami. The limitations of deep learning in adversarial settings. In *2016 IEEE European Symposium on Security and Privacy (EuroS&P)*, pages 372–387. IEEE, 2016. doi: 10.1109/EuroSP.2016.36.
- Guido F Montufar, Razvan Pascanu, Kyunghyun Cho, and Yoshua Bengio. On the number of linear regions of deep neural networks. In *Advances in Neural Information Processing Systems 27*, pages 2924–2932. Curran Associates, Inc., 2014. URL <http://papers.nips.cc/paper/5422-on-the-number-of-linear-regions-of-deep-neural-networks.pdf>.
- Shiqi Wang, Kexin Pei, Whitehouse Justin, Junfeng Yang, and Suman Jana. Efficient formal safety analysis of neural networks. In *32nd International Conference on Neural Information Processing Systems, NIPS’18*, page 6369–6379, Red Hook, NY, USA, 2018a. Curran Associates Inc. URL <http://papers.nips.cc/paper/7873-efficient-formal-safety-analysis-of-neural-networks.pdf>.
- Krishnamurthy Dvijotham, Robert Stanforth, Sven Gowal, Timothy A. Mann, and Pushmeet Kohli. A dual approach to scalable verification of deep networks. *CoRR*, abs/1803.06567, 2018b. URL <http://arxiv.org/abs/1803.06567>.
- Rüdiger Ehlers. Formal verification of piece-wise linear feed-forward neural networks. In *Automated Technology for Verification and Analysis*, pages 269–286. Springer, 2017. doi: 10.1007/978-3-319-68167-2_19.
- Guy Katz, Clark Barrett, David L. Dill, Kyle Julian, and Mykel J. Kochenderfer. Reluplex: An efficient smt solver for verifying deep neural networks. In *Computer Aided Verification*, pages 97–117. Springer, 2017. doi: 10.1007/978-3-319-63387-9_5.

- Alessio Lomuscio and Lalit Maganti. An approach to reachability analysis for feed-forward ReLU neural networks. *CoRR*, abs/1706.07351, 2017. URL <http://arxiv.org/abs/1706.07351>.
- Nina Narodytska, Shiva Kasiviswanathan, Leonid Ryzhyk, and Mooly Sagiv and. Verifying properties of binarized deep neural networks. In *32nd AAAI Conference on Artificial Intelligence*, 2018. URL <https://www.aaai.org/ocs/index.php/AAAI/AAAI18/paper/viewPaper/16898>.
- Luca Pulina and Armando Tacchella. An abstraction-refinement approach to verification of artificial neural networks. In *Computer Aided Verification*, pages 243–257. Springer, 2010. doi: 10.1007/978-3-642-14295-6_24.
- Eric Wong and Zico Kolter. Provable defenses against adversarial examples via the convex outer adversarial polytope. In *35th International Conference on Machine Learning*, volume 80 of *Proceedings of Machine Learning Research*, pages 5286–5295. PMLR, 2018. URL <http://proceedings.mlr.press/v80/wong18a.html>.
- Souradeep Dutta, Susmit Jha, Sriram Sankaranarayanan, and Ashish Tiwari. Output range analysis for deep feedforward neural networks. In *NASA Formal Methods*, pages 121–138. Springer, 2018. doi: 10.1007/978-3-319-77935-5_9.
- Matteo Fischetti and Jason Jo. Deep neural networks as 0-1 mixed integer linear programs: A feasibility study. *CoRR*, abs/1712.06174, 2017. URL <http://arxiv.org/abs/1712.06174>.
- Vincent Tjeng, Kai Xiao, and Russ Tedrake. Evaluating robustness of neural networks with mixed integer programming. *CoRR*, abs/1711.07356v3, 2019. URL <http://arxiv.org/abs/1711.07356v3>.
- Xiaowei Huang, Marta Kwiatkowska, Sen Wang, and Min Wu. Safety verification of deep neural networks. In *Computer Aided Verification*, pages 3–29. Springer, 2017. doi: 10.1007/978-3-319-63387-9_1.
- Lily Weng, Huan Zhang, Hongge Chen, Zhao Song, Cho-Jui Hsieh, Luca Daniel, Duane Boning, and Inderjit Dhillon. Towards fast computation of certified robustness for ReLU networks. In *35th International Conference on Machine Learning*, volume 80 of *Proceedings of Machine Learning Research*, pages 5276–5285. PMLR, 2018. URL <http://proceedings.mlr.press/v80/weng18a.html>.
- Wenjie Ruan, Xiaowei Huang, and Marta Kwiatkowska. Reachability analysis of deep neural networks with provable guarantees. In *27th International Joint Conference on Artificial Intelligence (IJCAI-18)*, pages 2651–2659. International Joint Conferences on Artificial Intelligence Organization, 2018. doi: 10.24963/ijcai.2018/368.
- Jianlin Li, Jiangchao Liu, Pengfei Yang, Liqian Chen, Xiaowei Huang, and Lijun Zhang. Analyzing deep neural networks with symbolic propagation: Towards higher precision and faster verification. In *International Static Analysis Symposium*, pages 296–319. Springer, 2019. doi: 10.1007/978-3-030-32304-2_15.
- Timon Gehr, Matthew Mirman, Dana Drachler-Cohen, Petar Tsankov, Swarat Chaudhuri, and Martin Vechev. AI²: Safety and robustness certification of neural networks with abstract interpretation. In *2018 IEEE Symposium on Security and Privacy (SP)*, pages 3–18. IEEE, 2018. doi: 10.1109/SP.2018.00058.
- Gagandeep Singh, Timon Gehr, Matthew Mirman, Markus Püschel, and Martin Vechev. Fast and effective robustness certification. In *Advances in Neural Information Processing Systems 31*, pages 10802–10813. Curran Associates, Inc., 2018. URL <http://papers.nips.cc/paper/8278-fast-and-effective-robustness-certification>.
- Gagandeep Singh, Timon Gehr, Markus Püschel, and Martin Vechev. An abstract domain for certifying neural networks. *Proc. ACM Program. Lang.*, 3(POPL), 2019. doi: 10.1145/3290354.
- Ian Goodfellow, Jonathon Shlens, and Christian Szegedy. Explaining and harnessing adversarial examples. In *International Conference on Learning Representations*, 2015. URL <http://arxiv.org/abs/1412.6572>.
- Shiqi Wang, Kexin Pei, Justin Whitehouse, Junfeng Yang, and Suman Jana. Formal security analysis of neural networks using symbolic intervals. In *27th USENIX Security Symposium*, pages 1599–1614. USENIX Association, 2018b. URL <https://www.usenix.org/conference/usenixsecurity18/presentation/wang-shiqi>.
- Yann LeCun, Corinna Cortes, and Christopher J.C. Burges. The MNIST database of handwritten digits, 2010. URL <http://yann.lecun.com/exdb/mnist/>.
- Diederik P. Kingma and Jimmy Ba. Adam: A method for stochastic optimization. In *3rd International Conference on Learning Representations (ICLR 2015)*, 2015. URL <http://arxiv.org/abs/1412.6980>.

Appendix

Performance of analyses averaged over all results

Table A.1: Performance of analyses averaged over all results						
Network	Software	Time [s]	Sub-analyses	Analysis result		
				adv.	non-adv.	undetermined
ff2x24	Neurify	4.7	141	770	222	8
	Debona 1.0	2.7	152	773	227	0
	Debona 1.1	2.1	119	773	227	0
ff2x50	Neurify	84.4	2,656	663	213	126
	Debona 1.0	123.5	6,581	671	238	91
	Debona 1.1	96.0	5,204	673	254	73
ff2x512	Neurify	3.8	58	252	11	737
	Debona 1.0	33.9	895	253	16	731
	Debona 1.1	94.0	2,191	224	57	719
ff3x24	Neurify	17.7	454	603	371	26
	Debona 1.0	10.0	448	608	391	1
	Debona 1.1	7.6	335	608	391	1
ff3x50	Neurify	132.5	3,648	561	215	224
	Debona 1.0	192.4	7,746	561	255	184
	Debona 1.1	148.6	6,455	558	289	153
ff5x24	Neurify	95.3	2,543	677	244	79
	Debona 1.0	131.6	3,425	689	262	49
	Debona 1.1	96.5	3,271	693	272	35

Similar to Table 1, Table A.1 provides the average runtime of each software version over the different network architectures. However, Table A.1 reports the average over all analyses that returned a result, not only the subset that was analyzable by all implementations. The increase in runtime and number of sub-analyses for Debona 1.0 and 1.1 is to be expected, as they include analyses that result in a timeout for previous software versions.

Tightness of initial output bounds

Table A.2: Tightness of initial output bounds		
Network	Software	Average bound distance
ff2x24	Neurify	24.0
	Debona 1.0	24.0
	Debona 1.1	21.2
ff2x50	Neurify	45.1
	Debona 1.0	45.1
	Debona 1.1	37.7
ff2x512	Neurify	252.1
	Debona 1.0	252.1
	Debona 1.1	191.1
ff3x24	Neurify	13.7
	Debona 1.0	13.7
	Debona 1.1	12.1
ff3x50	Neurify	25.1
	Debona 1.0	25.1
	Debona 1.1	20.1
ff5x24	Neurify	27.1
	Debona 1.0	27.1
	Debona 1.1	24.2

Table A.2 lists the average distance between the upper and lower bounds of the output nodes, averaged over all 1,000 test images and all 10 output nodes. Neurify and Debona 1.0 have the exact same average distance, as Debona 1.0 is only a re-implementation of Neurify, and none of the removed bugs influenced the bounds that are computed before any splitting is performed.